ORIGINAL PAPER

Effects of large-scale climate patterns and human activities on hydrological drought: a case study in the Luanhe River basin, China

Yixuan Wang · Jianzhu Li · Ping Feng · Fulong Chen

Abstract Evaluation of the impact of climate variability and human activities on hydrological drought is of great significance for drought mitigation strategies. In this study, standardized runoff index (SRI) at various time scales is used to characterize hydrological droughts in the Luanhe River basin, northeast of China, for the period of 1959–2011. Correlation analysis is conducted to examine the associations between the hydrological droughts and large-scale oceanic–atmospheric patterns (AMO and ENSO). Climate-induced and human-induced influence indices are also developed based on standardized precipitation index and SRI to investigate the possible influences of the climate patterns and human activities on the hydrological droughts. Results indicate that the significant influence of AMO on hydrological drought at different time scales is evident among different months across the Luanhe River basin, with warm (cold) AMO phases favoring drought (wet) conditions. The direct linkage of ENSO to hydrological drought is relatively weak in the basin, while the extent of the linkage can be improved with increasing time lags. Moreover, El Niño phases show a closer relation with the drought events of the region as compared with La Niña phases. It is also implied that human activities exhibit aggravating effects on hydrological drought at shorter time scales over the basin, whereas they might show mitigating effects at longer time scales in some areas of the basin. These findings can be beneficial for better understanding how the hydrological drought responses to climate changes and human activities, thereby providing valuable references for drought forecasts and water resources managements in the Luanhe River basin.

Keywords Hydrological drought · Standardized runoff index · El Niño/southern oscillation · Atlantic multidecadal oscillation · Human activities

Y. Wang · J. Li (✉) · P. Feng · F. Chen
State Key Laboratory of Hydraulic Engineering Simulation and Safety, Tianjin University,
Tianjin 300072, China
e-mail: lijianzhu@tju.edu.cn

F. Chen
College of Water Conservancy and Architectural Engineering, Shihezi University,
Shihezi 832003, Xinjiang, China

Springer

1 Introduction

Drought, as a complex, creeping natural phenomenon, is generally related to a sustained and spatially extensive occurrence of insufficient water availability for supplying socio-economic activities and natural ecosystems (Beran and Rodier 1985; Hosseinzadeh Talaee et al. 2012). When a drought event occurs, moisture deficits are observed in all components of the water cycle (Dracup et al. 1980; Van Huijgevoort et al. 2012). Hydrological drought refers to a significant decrease in water resource in all its forms appearing in the land phase of the hydrological cycle (Nalbantis and Tsakiris 2009). As the high dependence of many activities (e.g., irrigation and industrial consumption) on surface water and/or groundwater supply, hydrological drought is considered as the most important one among different types of droughts (Vasiliades et al. 2011; Li et al. 2013). Considering the varying response time of water deficit to climatic condition and human exploitation, the hydrological drought exhibits diverse temporal scales, namely inconsistent drought characteristics may emerge for the same condition of insufficient moisture at different time scales (Shukla and Wood 2008; Kao and Govindaraju 2010).

Accordingly, it is important to examine and analyze the multiple status of hydrological drought over various time scales. Based on the concept of the standardized precipitation index (SPI), the standardized runoff index (SRI) has been proposed as a useful counterpart for depicting hydrological aspects of drought (Shukla and Wood 2008). This drought index not only allows comparisons of hydrological drought severity across time and space, but also can be calculated at varying time scales according to the needs of water resource managements (Li et al. 2013; Sol'áková et al. 2013). What is more, the runoff-based SRI presents a simple and efficient measure for hydrological drought study as its incorporate information of both meteorological conditions and human activities in a region (Wen et al. 2011).

Under the background of global climate changes and local anthropogenic intensification, general consensus support that many regions of the world have suffered from more frequent and severe drought events in recent decades (Ye et al. 2013; Chen and Yang 2013).

The anomalies of climate can be traced to large-scale oceanic–atmospheric patterns, such as the Atlantic multidecadal oscillation (AMO) and the El Niño/southern oscillation (ENSO) (Fraedrich and Müller 1992; Enfield et al. 2001). Many researchers have documented that the variability of the hydrological drought in both spatial and temporal dimensions can be explained in terms of climate signals (Stahl and Demuth 1999; Bradbury et al. 2002; Özger et al. 2009; Hosseinzadeh Talaee et al. 2012).

The AMO is a recent label for a climate oscillation in the North Atlantic with a period of 65–80 years (Kerr 2000). Previous studies have revealed that the AMO could exert direct influences on the regional climate and drought (Sutton and Hodson 2005; Knight et al. 2006; Mo et al. 2009). It has been reported that the warm-phase AMO favors warmer winters in much of China, with enhanced precipitation in northern China, while reduced precipitation in the south, and vice versa (Lu et al. 2006b; Li and Bates 2007; Li et al. 2009; Wang et al. 2009). Nevertheless, there is little evidence on the impact of the AMO on hydrological drought in China.

ENSO, as the dominant coupled ocean–atmosphere mode of the tropical Pacific, has significant impacts on the hydrological processes and drought characteristics over China (Jiang et al. 2006; Wang et al. 2006; Tang and Yuan 2010; Wang et al. 2013). Generally, the warm phases of ENSO (El Niño) are directly correlated with the major drought events

in northern China, although the intensity of the correlation varies with the region (Chen et al. 1995; Su and Li 2012; Ouyang et al. 2014). Lu et al. (2006a) analyzed the association between the drought severity of different areas in China and ENSO index and found that the drought condition of North China presents the most sensitive response to the El Niño events.

In addition to climate change, understanding the effect of human activities on hydrological drought has also drawn considerable concerns with the rapid development of economics and society. Human activities, mainly including urbanization, agricultural practices, human-induced land use changes and construction of hydraulic structures, can lead to changes in hydrological regime, which eventually affect the hydrological drought (Zhang et al. 2012; Song et al. 2013; Xing et al. 2013). For instance, the increased concentration of greenhouse gases in the atmosphere due to expanded population can contribute to global warming, and consequently, result in exacerbating the regional drought severity (Nicholls 2004; Kirono et al. 2011). The land degradation or deforestation caused by extensive urbanization, generally leads to reduction in water yield at catchment scale, thereby elevating the hydrological drought in the related area (Niehoff et al. 2002; Di Rita and Magri 2009). Although the hydrological project (such as reservoir operation and water diversion) has capability of reallocating the water storage for a basin to cope with drought events, it could also be responsible for the aggravation of hydrological drought in the basin (López-Moreno et al. 2009; Wen et al. 2011; Li et al. 2013). The impact of regional human
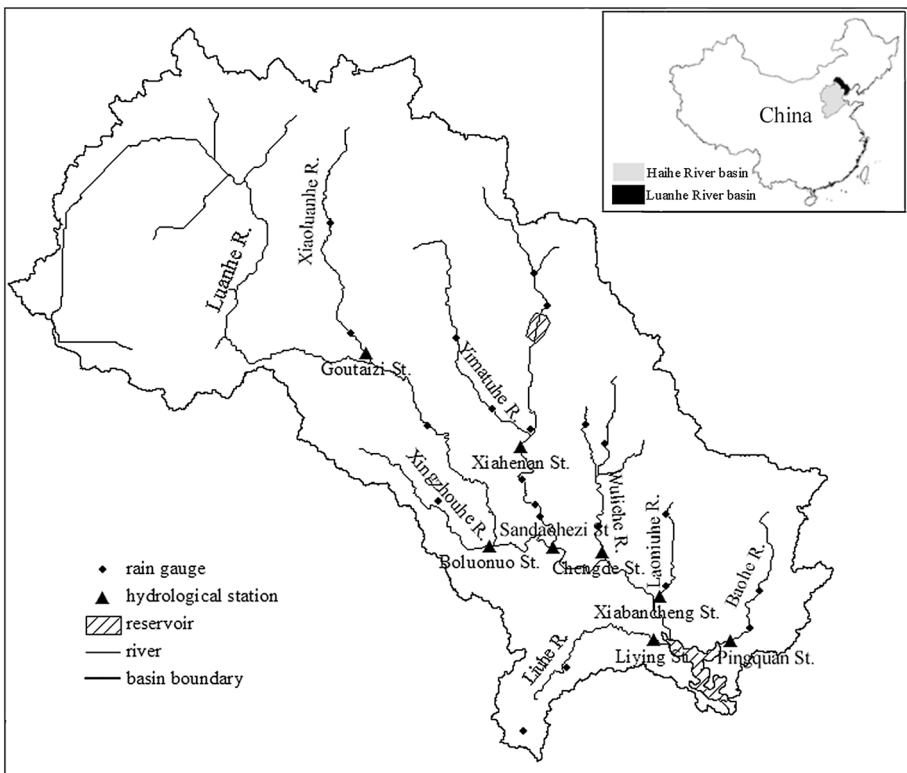

Fig. 1 Location of the Luanhe River basin and the selected stations

activities on hydrology drought obviously varies with time scale, whereas the impacts at different time scales have received only limited attention.

The Luanhe River basin is of great significance for water supply to Tianjin, the largest opening coastal city of North China. In recent years, the frequent occurrence of drought events has resulted in serious environmental degradation and water crises in the region. To date, some studies discussing the response of hydrological variables (such as temperature, precipitation and runoff) to climatic and human-induced changes have been carried out for the basin (Wang and Wang 2009; Wang et al. 2013; Zeng et al. 2014); however, information about the impacts of these changes on hydrological drought at various time scales is not available. Evaluation of the possible influence of large-scale climate patterns on hydrological drought is of great importance for drought forecast and mitigation, by considering the evolution of the climatic signals. Additionally, in order to ensure sustainable water resources utilization and development, it is important to understand the response of hydrological drought to regional human activities at different time scales. The main purpose of this study was to investigate the effects of climate change and regional human activities on hydrological drought at both shorter and longer time scales, and expect to provide significant information for drought forecasts and water resources managements in the Luanhe River basin.

2 Study area and data

2.1 Study area

The Luanhe River basin is located at the northeast part of China (Fig. 1). It extends from 115°30′E to 119°15′E longitude and 39°10′N to 42°30′N latitude with a total drainage area of 33,700 km^2. The elevation within the basin ranges from 2 to 2,205 m and averages 766 m. Among the entire area, the topography significantly descends from northwest to southeast, and mountainous regions account for nearly 98 % of the area, while plains account for about 2 %. The basin is in a temperate semiarid continental monsoon climate, with an annual average temperature of −0.3 to 11 °C, an annual average precipitation of 400–700 mm, and an annual average potential evapotranspiration of 950–1,150 mm.

The spatial and temporal distribution of the precipitation within the Luanhe River basin is uneven, and about 70–80 % of the annual precipitation falls in the rainy months of June to September. The region receives an average runoff of 4.69 billion cubic meters per year. Floods in the basin are often caused by rainstorms and occur in July and August. As the short duration and high intensity of the rainstorms, the flood is of high peak and large amount and with the duration between 3 and 6 days. Land use types in the area are forest, grassland, urban land, agricultural and unutilized land. Due to rainfall reduction and soil and water conservation, the average annual runoff had decreased by 30 % after 1980 (Li and Feng 2007).

The Luanhe River basin is well known for water supply function for the Tianjin city, an important metropolis of China. It was planned to introduce water of a billion cubic meters to Tianjin per year from the basin. However, the actual amount of water transferred to Tianjin was less than the plan in several years, especially in the last decade. The deficient water supply to Tianjin is mainly resulted from the consecutive drought in the twenty-first century. The drought events in the basin mainly occurred in 1961, 1963, 1968, 1972, 1980–1984, 1997–2005, 2007 and 2009, especially more severe during the last decade

(Ma et al. 2013; Yang et al. 2013).The long-lasting drought aggravated environmental degradation and water crisis in Tianjin city.

In this study, eight sub-basins (i.e., Luanhe, Wuliehe, Baohe, Xiaoluanhe, Yixunhe, Laoniuhe, Xingzhouhe and Liuhe) in the Luanhe River basin were selected as the study area (Fig. 1). The sub-basins range in area from 626 to 17,100 km^2, and each with a hydrological station (Sandaohezi, Chengde, Pingquan, Goutaizi, Xiahenan, Xiabancheng, Boluonuo and Liying, respectively) at the outlet.

2.2 Data

According to the length and continuity of available records, monthly runoff data of eight hydrological stations from 1959 to 2011 were prepared, and the same-period time series of monthly rainfall were obtained from 21 rain gauges distributed in each sub-basin. The locations of the selected stations are given in Fig. 1. All the data were provided by Hydrology and Water Resource Survey Bureau of Hebei Province.

Two climatic indices were employed in this study to represent the states of large-scale climate patterns. The first climatic index is the AMO index (AMOI) which is defined as the detrended, regionally averaged, summer sea surface temperatures (SSTs) anomalies over the North Atlantic Ocean (0–60°N, 7.5–75°W) (Enfield et al. 2001). During AMO warm (cold) phases, the AMOI over the entire North Atlantic show positive (negative) anomalies. The monthly AMOI is taken from the NOAA Earth System Research Laboratory. The second climatic index is the SOI which characterizes the interannual ENSO state. The Troup SOI (Troup 1965) is defined as ten times the standardized anomaly of the mean sea level pressure (MSLP) difference between Tahiti, Society Island and Darwin, Australia. Large negative values of the SOI indicate periods of El Niño, while large positive values indicate periods of La Niña. The monthly Troup SOI series used here was obtained from the National Climate Centre of the Australian Bureau. Subsequently, only the 1959–2011 period was used in the study to match the runoff data.

3 Method

3.1 Standardized runoff index

This study focused on the hydrological drought defined by standardized runoff index (SRI) which is statistically similar to the well-known standardized precipitation index (SPI) (Shukla and Wood 2008). In order to reduce the degree of auto-correlation among samples and alleviate the effect of seasonal variability in an appropriate manner, the procedure for calculating the SRI includes the following steps (Kao and Govindaraju 2010).

(1) Let $R(t)$ represent the monthly runoff measured at time t. The average values $Y_w(t) = \sum_{i=t-w+1}^{t} R(i)/w$ indicate the mean discharge for a given w-month time scale with respect to t. (2) Let m represent the specified month, i.e., January, February,…, November, October (denoted as Jan, Feb,…, Nov, Oct). The subset Y_{w-m} is defined by grouping Y_w based on its ending month m. In doing so, samples within the same group Y_{w-m} will be subject to the same seasonal effect. Each of the subsets is fitted to a suitable probability distribution, then obtaining the cumulative probability u_{w-m} of Y_{w-m}. (3) The cumulative probability u_{w-m} is converted to a standard normal deviate (with zero mean and unit variance) by using an equal probability transformation (Bordi and Sutera 2001; Shukla and

Wood [2008]). This value is the SRI$_w$ for the particular w-month average runoff. Positive values of the SRI reflect wet conditions, while negative values indicate dry conditions. Table 1 shows the range of SRI values along with their classifications.

The SRI has the advantages that it is interpretable for probabilistic analysis and can be compared easily across space and time. Using the SRI as the indicator, a functional and quantitative definition of hydrological drought can be established at an arbitrary time scale. McKee et al. (1993) defined a drought event as a period in which the SPI is continuously negative and reaches a value of −1.0 or less. In this study, a hydrological drought event was characterized by drought magnitude and duration simultaneously. Drought duration denoted by D is the continuously negative SRI periods without any SRI larger than −1.0. Drought magnitude denoted by M is the cumulative values of the SRI within the drought duration. For convenience, drought magnitude is taken to be positive and defined by (Mckee et al. 1993):

$$M = - \sum_{i=1}^{D} \text{SRI}_w(i) \tag{1}$$

where i starts with the first month of a drought event and continues until the end of the drought.

3.2 Correlation analysis

There are two tests commonly used to evaluate the strength of the association between two variables: Kendall's rank correlation and Spearman's rank correlation. Both of the tests are nonparametric, namely they are not necessary to assume that the variables are normally distributed. However, the Kendall test might be preferable to use rather than the Spearman test as the "Kendall correlation measure is more robust and slightly more efficient than the Spearman's rank correlation" (Croux and Dehon 2010). Based on the consideration, Kendall's rank correlation was employed in this study.

Kendall's rank correlation (also called Kendall's τ) is a nonparametric rank-based test that measures the strength of monotonic correlation, whether linear or nonlinear, between two observations x_i and y_i associated with variables X and Y. Kendall's rank correlation coefficient, τ, is expressed as:

$$\tau = \frac{\sum_{i<j} \left(\text{sign}(x[j] - x[i]) \times \text{sign}(y[j] - y[i]) \right)}{n(n-1)/2} \tag{2}$$

where n is the number of observations in each time series. The Kendall's τ coefficient takes a value between −1 and +1. A positive coefficient indicates increasing trend and vice

Table 1 SRI classification

SRI	Classification
>2	Extremely wet
1.5–2.0	Very wet
1.0–1.5	Moderately wet
−1.0 to 1.0	Near normal
−1.5 to −1.0	Moderately dry
−2.0 to −1.5	Severely dry
−2.0 and less	Extremely dry

versa. A correlation of +1 or −1 occurs when each of the variables is a perfect monotone function of the other, and a correlation close to zero means there is no relationship between the variables. In addition, the square of the correlation, which is defined as the coefficient of determination, can be used as a measure of the proportion of variability that two variables share, or how much one can be explained by the other (Bolboaca and Jäntschi 2006; Hosseinzadeh Talaee et al. 2012).

3.3 Climate-induced influence indices

Kim et al. (2006) proposed conceptual indices based on SPI to quantifying the strength of linkages between climate patterns and precipitation variability in the Colorado River basin. The concepts of these conceptual indices were applied in defining climate-induced influence indices in this study. The climate-induced influence indices were developed based on SPI to detect the possible influences of climate patterns on regional drought condition. The indices, including influence frequency (I_F) and influence intensity (I_I), are calculated as follows:

$$I_F = \frac{N_d}{N_c} \tag{3}$$

$$I_I = \frac{1}{N_c} \sum_{i=1}^{N_c} \mathrm{SPI}_w(i) \tag{4}$$

where N_d is the number of months with the SPI_w less than −1.0 during a climate phase, N_c is the number of months in the climate phase, and $\mathrm{SPI}_w(i)$ is the value of SPI on w-month time scale corresponding to month i. A larger I_F means a closer relation between the specified climate phase and drought events. A positive (negative) I_I indicates that the climate phase favors wetness (drought).

3.4 Human-induced influence indices

In this study, meteorological drought was derived from the precipitation-based SPI and hydrological drought was quantified by the runoff-based SRI. The meteorological drought based on precipitation deficits is purely dependent on climate anomalies (McKee et al. 1993), whereas the hydrological drought related to runoff deficits is the comprehensive result of climatic anomalies and human activities (Shukla and Wood 2008).

For the river basin that has undergone intensive anthropogenic disturbances, a response in runoff will occur and the change will be gradual or abrupt (Li et al. 2007; Zhao et al. 2009; Zhang et al. 2013). Consequently, it is reasonable to assume that changes in hydrological drought might be coincident with those exhibited in runoff. Double cumulative curve (DCC) is frequently used in paired variables to detect hydrological changes caused by human activities (Searcy and Hardison 1960). In this study, the precipitation-runoff DCC was adopted to identify the change-point of runoff series; meanwhile, this change-point was regarded as the approximate time when human activities imposed influences on hydrological drought. Subsequently, the whole time period was divided into two periods. The first one is before the change-point, called the ''natural period,'' which represents the baseline with no significant human activities. The second one after the change-point is called the ''impact period,'' in which there is a notable change associated with both human activities and climate change in hydrological drought.

In consideration of the definition of drought event, special attentions were paid on the drought index less than -0.1, referred to as SPI′ or SRI′ hereinafter. To understand the changing trend of drought, the change ratios of the meteorological and hydrological drought, denoted as R_P and R_R, respectively, are defined by

$$R_P = \frac{\left|\overline{SPI'_I}\right| - \left|\overline{SPI'_N}\right|}{\left|\overline{SPI'_N}\right|} \tag{5}$$

$$R_R = \frac{\left|\overline{SRI'_I}\right| - \left|\overline{SRI'_N}\right|}{\left|\overline{SRI'_N}\right|} \tag{6}$$

where the $\overline{SPI'_N}$ and $\overline{SPI'_I}$, $\overline{SRI'_N}$ and $\overline{SRI'_I}$ represent the means of the SPI′ and SRI′ in the natural and impact period, respectively. $R_P > 0$ suggests that climate anomalies, mainly related to precipitation variations, accentuate the severity of droughts. $R_R > 0$ suggests an aggravating trend of the hydrological drought, which is a consequence of climate changes and human activities.

In order to evaluate the effect of human activities on hydrological drought, human-induced influence index was proposed, based on the assumption that the degree of hydrological drought change caused by climate anomalies (precipitation variability) is identical with that of meteorological drought. Accordingly, the noticeable difference between the R_R and R_P emerges as a consequence of human-induced impacts. The human-induced influence index denoted as ΔR is given by the following expression:

$$\Delta R = R_R - R_P \tag{7}$$

$\Delta R > 0$ indicates the aggravating effect of human activities on hydrological drought severity; $\Delta R < 0$ indicates the mitigating effect; the larger the value, the more significant the effect.

4 Results

4.1 Hydrological droughts at various time scales

The monthly runoff records of the hydrological stations were reformatted as different time scale runoff series to calculate SRI. In this study, 1-, 3-, 6- and 12-month time scales were selected. Although the two-parameter gamma distribution was suggested by McKee et al. (1993) for computing SPI, it may be unsuitable for the SRI. In order to test the appropriateness of three distributions (two-parameter gamma, generalized extreme value and Pearson Type III) considered in this study, Kolmogorov–Smirnov test was applied for the goodness of fit at the 1 % significance level, with the parameters estimated by maximum likelihood method. The results indicated that the Pearson Type III distribution provides the best fits for most cases (>90 % for each monthly runoff series). This is in agreement with the previous studies (Xiong and Guo 2004; Li et al. 2013), which have demonstrated that the Pearson Type III distribution is the best one for fitting the river discharge series in China. Therefore, the Pearson Type III distribution was selected for calculating the SRI.

Any assessment of drought and its impacts requires a specific time scale, since drought initiation, duration, severity and other drought variables are all dependent on time scales (McKee et al. 1993). The 1- and 12-month SRI series of the period 1959–2011 at Chengde

station are illustrated in Fig. 2 as an example. Generally, the series of SRI at shorter time scales have greater fluctuation, resulting in high-frequency drought events with shorter drought durations. While the SRI_{12} series exhibited smooth variation, indicating that the droughts at longer time scales are less frequent, but lasted longer.

Hydrological drought events were then abstracted using the definition mentioned previously. In addition, the ratio between the number of months with SRI less than −1 and the total number of months counted for the sample series was represented as arrival rate in this study.

The arrival rates and some basic statistics of the drought events for each hydrological station and each time scale are given in Table 2.

For all the stations, the drought arrival rates decreased with increasing SRI time scales, and the station associated with more frequent occurrence of droughts generally had shorter drought duration and smaller drought magnitude. At shorter time scales, the highest frequent occurrence of drought events was observed at Xiahenan station, and both the mean drought duration and mean drought magnitude of Pingquan station were greater than those of other stations. On the other hand, for longer time scales, Xiabancheng station had the longest mean drought durations and maximum mean drought magnitude, meanwhile the drought arrival rate of Goutaizi station was ranked first among the eight stations.

On 1-month time scale, the most severe hydrological drought event, which was observed at Pingquan station, started from February 2007 with a magnitude of 36.14 and a duration of 23 months. Furthermore, the greatest drought magnitude of 83.77 and the longest duration of 57 months occurred simultaneously at Xiabancheng station. The corresponding drought event defined by the SRI_{12} spanned the period of September 2006 to May 2011. These results prove the findings of Li and Feng (2007), which suggested that the drought conditions in the Luanhe River basin have become more severe during the last decade.

The 1972 drought event was evident in all four sets of the SRI series for most stations. The extreme hydrological drought events in 2000 and 2009 were validated through the inspection of SRI_1 at all the stations, with the peak intensities averaged over the eight stations equal to −2.15 and −2.29, respectively. Based on the series of SRI_{12}, a long-term drought starting in the summer of 2002 was identified at all the stations, of which the duration ranged from 15 to 37 months and averaged 27 months. Moreover, during 1980–1984, all of the stations experienced at least one severe drought event persisting for more than 12 months. These results are in agreement with the historical records and previous studies related to drought events in the Luanhe River basin (Ma et al. 2013; Yang et al. 2013; Feng et al. 2014).

4.2 Linkage between large-scale climate patterns and hydrological drought

To evaluate the association between climate patterns and hydrological drought in the Luanhe River basin, Kendall's τ correlation test was performed between the climate indices and the SRI of the eight hydrological stations at the 5 % significant levels.
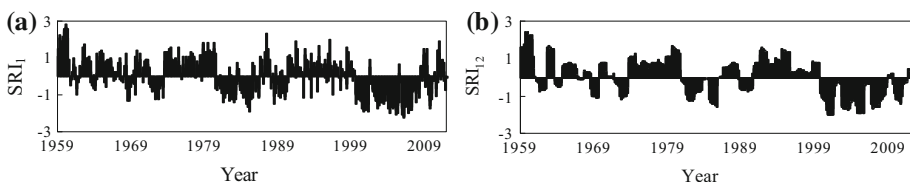

Fig. 2 **a** 1-month and **b** 12-month SRI series of the period 1959–2011 at Chengde station

Table 2 Basic statistics of drought events for the selected hydrological stations in the Luanhe River basin

Station	Sandaohezi	Chengde	Pingquan	Goutaizi	Xiahenan	Xiabancheng	Boluonuo	Liying
1-month								
Arrival rate	0.47	0.49	0.30	0.47	0.58	0.40	0.53	0.49
M								
Min	1.03	1.00	1.03	1.01	1.03	1.01	1.00	1.00
Max	19.00	24.63	36.14	10.10	22.12	30.37	22.94	19.73
Mean	3.47	5.00	8.33	2.76	3.27	6.24	4.11	5.11
SD	3.85	6.41	10.55	1.97	3.80	8.68	4.51	5.54
D								
Min	1	1	1	1	1	1	1	1
Max	11	16	23	6	11	17	11	12
Mean	2.20	3.50	5.90	1.80	2.12	4.07	2.78	3.42
SD	2.17	4.11	7.14	1.19	2.12	4.91	2.43	3.42
3-month								
Arrival rate	0.38	0.28	0.19	0.38	0.43	0.25	0.36	0.38
M								
Min	1.02	1.14	1.02	1.03	1.02	1.00	1.01	1.00
Max	30.52	34.01	36.90	32.83	31.78	47.10	32.09	29.40
Mean	6.08	10.15	14.34	6.39	5.44	13.10	7.54	7.91
SD	6.88	10.27	15.33	7.10	7.03	15.95	7.45	8.11
D								
Min	1	1	1	1	1	1	1	1
Max	15	22	24	18	15	28	18	22
Mean	4.00	6.82	9.92	4.08	3.52	8.62	5.09	5.32
SD	3.49	6.25	9.66	3.89	3.78	9.81	4.30	5.45
6-month								
Arrival rate	0.32	0.26	0.15	0.34	0.26	0.11	0.25	0.28
M								
Min	1.00	1.02	1.01	1.00	1.03	3.09	1.05	1.03
Max	37.97	35.15	42.39	32.71	48.19	60.88	34.42	35.47
Mean	8.65	13.01	18.95	7.22	9.30	28.64	12.72	11.66
SD	10.32	12.36	17.13	8.54	14.02	22.27	11.12	11.84
D								
Min	1	1	1	1	1	3	1	1
Max	19	22	28	16	34	38	20	25
Mean	5.89	8.93	12.67	4.68	6.12	18.83	8.38	8.00
SD	5.85	7.51	10.42	4.67	8.85	13.23	6.05	7.81
12-month								
Arrival rate	0.13	0.15	0.11	0.21	0.17	0.06	0.13	0.15
M								
Min	12.18	7.60	3.09	1.00	1.15	35.78	3.41	7.38
Max	53.09	58.84	44.01	44.14	83.41	83.77	60.22	39.01
Mean	25.13	23.44	27.09	11.95	17.25	59.90	23.29	24.11
SD	15.97	17.00	18.44	12.81	26.24	23.82	18.30	12.35

Table 2 continued

Station	Sandaohezi	Chengde	Pingquan	Goutaizi	Xiahenan	Xiabancheng	Boluonuo	Liying
D
Min	10	7	3	1	1	25	3	7
Max	37	36	30	25	50	57	37	25
Mean	17.29	16.38	17.50	8.00	11.11	39.67	15.29	16.88
SD	9.69	9.35	11.10	7.14	15.45	16.17	10.48	7.55

The unit of drought duration (D) is 1 month

SD standard deviation, *Max* maximum, *Min* minimum

Corresponding to the time scales selected for the SRI, time series used to represent climatic patterns were composed based on monthly values and 3-, 6-, 12-month moving averages of the associated indices, denoted as $AMOI_1$ and SOI_1, $AMOI_3$ and SOI_3, $AMOI_6$ and SOI_6, $AMOI_{12}$ and SOI_{12}, respectively. In addition, the lead times of 3, 6 and 12 months were considered herein to investigate lag correlations between the SRI and the prior climatic indices.

4.2.1 AMO phenomenon

The results of Kendall's τ test between SRI and AMOI for each month are presented in Table 3.

$AMOI_1$ and SRI_1 As shown in Table 3, six out of the eight stations exhibited significant negative correlations between their SRI_1 and the simultaneous $AMOI_1$ in July, as well as August. These correlations were in the range of -0.30 to -0.43, indicating that about 9–18 % of variance in these drought severity patterns is associated with the concurrent AMO forcing. All lag correlations between the SRI_1 and the prior $AMOI_1$ were found to be negative. At both 3- and 6-month lagged stages, the greatest number of significant correlations was observed in July. Furthermore, about 90 % of the SRI_1 in August and September had significant correlations with the 12-month leading $AMOI_1$. In general, the August SRI_1 yielded the greatest correlation with the 12-month prior $AMOI_1$, where the significant correlations averaged -0.47.

$AMOI_3$ and SRI_3 The $AMOI_3$ from August to October had significant negative correlations with the synchronous SRI_3 at 75 % of the stations. Among the above correlations, the greatest one of -0.40 was found in September at Xiahenan station. From July to September, about 60 % of the SRI_3 showed significant negative correlations with both the 3- and 6-month leading $AMOI_3$. Moreover, about 90 % of the stations exhibited significant correlations between the 12-months leading $AMOI_3$ and the SRI_3 from August to November. As a whole, the strongest correlation was found between the October SRI_3 and the $AMOI_3$ of prior 12 months, where the average of significant correlations reached -0.47 and the greatest one of -0.56 was found at Xiahenan station.

$AMOI_6$ and SRI_6 From August to October, significant concurrent correlations between SRI_6 and $AMOI_6$ were found at 75 % of the stations, of which the greatest one of -0.46 was observed in July at Xiabancheng station. It means that about 21 % of the variance of the July SRI_6 at Xiabancheng station is associated with the simultaneous AMO forcing. In regard to the time lags of both 3 and 6 months, more than 60 % of the SRI_6 from July to November had significant negative correlations with the prior $AMOI_6$. Additionally, about 90 % of the 12-month lag correlations were observed to be significant negative from August to December. Among the lag correlations, the strongest correlation of -0.56 was

Table 3 Number of stations with a significant correlation between AMOI and SRI for each time scale and each lead time

Correlation	Lead time	Jan	Feb	Mar	Apr	May	Jun	Jul	Aug	Sep	Oct	Nov	Dec
$AMOI_1$ and SRI_1	Concurrent	0	−2	−4	0	0	0	−6	−6	−1	−1	−2	−1
	3 months	−3	−2	−3	0	0	0	−6	−3	−2	−2	−4	−2
	6 months	−3	−4	−4	−3	0	0	−5	−3	−4	−2	−2	−1
	12 months	−3	−2	−5	−1	0	−1	−5	−7	−7	−4	−4	−3
$AMOI_3$ and SRI_3	Concurrent	−1	−0	−2	−2	0	0	−4	−6	−6	−6	−2	−2
	3 months	−2	−2	−2	−2	0	0	−5	−5	−6	−4	−2	−2
	6 months	−1	−2	−2	−2	−2	0	−5	−5	−5	−4	−2	−2
	12 months	−2	−1	−2	−1	−2	−1	−6	−7	−7	−7	−7	−4
$AMOI_6$ and SRI_6	concurrent	−2	−2	−2	−2	0	0	−5	−6	−6	−6	−5	−5
	3 months	−3	−2	−2	−3	−1	−1	−5	−5	−5	−6	−6	−6
	6 months	−3	−2	−2	−3	−2	−3	−6	−6	−6	−5	−5	−4
	12 months	−6	−5	−3	−2	−1	−1	−6	−7	−7	−7	−7	−7
$AMOI_{12}$ and SRI_{12}	Concurrent	−2	−2	−2	−2	−1	−1	−3	−4	−6	−6	−6	−6
	3 months	−6	−6	−6	−5	−5	−5	−6	−6	−6	−6	−6	−6
	6 months	−6	−5	−5	−5	−6	−6	−6	−6	−6	−6	−6	−6
	12 months	−7	−7	−7	−6	−6	−6	−5	−7	−7	−7	−7	−7

The negative number means the there are the corresponding number of stations exhibited significant negative correlations, while the positive number means significant positive correlations

found between the August SRI_6 and the $AMOI_6$ with 12-month lead time at Chengde station.

$AMOI_{12}$ and SRI_{12} From September to December, 75 % of the stations had significant concurrent correlations between SRI_{12} and $AMOI_{12}$. These significant correlations were in the range of −0.25 to −0.46, of which the strongest one was found in October at Xiabancheng station, suggesting that roughly 21 % of the variance of October drought severity in the Laoniuhe sub-basin can be explained by the concurrent AMO anomalies. For all the considered lead times, more than 60 % of lag correlations were proved to be significant negative all year around. Additionally, the strongest association occurred between the September SRI_{12} and the 12-month leading $AMOI_{12}$, with significant correlations ranging from −0.31 to −0.63 and averaging −0.46.

Overall, the results indicate that the significant influence of AMO on hydrological drought is evident across the Luanhe River basin. With respect to the hydrological droughts at 1-month time scale, the potential teleconnection of AMO mainly occurs in July and August. For 3-month time scale, the impact of AMO on the hydrological droughts is significant in flood season (July through October). As to 6-month time scale, the existence of AMO teleconnection with the hydrological droughts is revealed in the second half of the year (July through December). The hydrological droughts at 12-month time scale are generally affected by the variability of AMO all year around. Moreover, as the time lag increases, the strength of the relationship between prior AMO signal and hydrological drought severity becomes greater in the basin.

4.2.2 ENSO phenomenon

Monthly Kendall's τ correlations between SRI and SOI are listed in Table 4.

SOI$_1$ and SRI$_1$ All concurrent correlations between the SRI$_1$ and the SOI$_1$ were relatively weak, and only a few number of stations exhibited significant correlations between the SRI$_1$ and the 3-month prior SOI$_1$. However, at 6-month lagged stage, there is a significant negative correlation between the August SRI$_1$ and the February SOI$_1$ at seven stations. For time lags of 12 months, a significant negative correlation was observed between the October SRI$_1$ and the prior SOI$_1$ at five stations. Among the correlations, the strongest one of −0.49 was found between the February SRI$_1$ and the 12-month leading SOI$_1$ at Boluono station.

SOI$_3$ and SRI$_3$ In regards to all the SRI$_3$ series, none of the selected stations presented a significant correlation with the synchronous SOI$_3$, and scarcely any stations showed significant relationships with the prior 3-month SOI$_3$. In addition, 75 % of the October SRI$_3$ yielded significant negative correlations with the May SOI$_3$. From November to February, the SRI$_3$ were significantly correlated with the 12-month leading SOI$_3$ at 75 % of the stations, with the correlation coefficients in the range of −0.27 to −0.46.

SOI$_6$ and SRI$_6$ The Kendall's τ test did not identify any significant associations between SRI$_6$ and concurrent SOI$_6$. For the time lags of both 3 and 6 months, just a few stations exhibited significant lag correlations. Additionally, about 90 % of the SRI$_6$ in January and February had significant correlations with the 12-month leading SOI$_6$. At the 12-month lagged stage, the strongest relationship was found in February, where the correlation averaged over the eight stations was about −0.35 and the highest one of −0.46 was found at Boluono station.

SOI$_{12}$ and SRI$_{12}$ As shown in Table 4, the amount of significant correlations between SRI$_{12}$ and SOI$_{12}$ was relatively low, for all the concurrent and lag correlations. However,

Table 4 Number of stations with a significant correlation between SOI and SRI for each time scale and each lead time

Correlation	Lead time	Jan	Feb	Mar	Apr	May	Jun	Jul	Aug	Sep	Oct	Nov	Dec
SOI$_1$ and SRI$_1$	Concurrent	0	0	0	0	0	+1	0	0	0	0	0	0
	3 months	+1	0	0	0	0	0	−1	0	+1	0	0	0
	6 months	+1	0	0	0	0	0	0	−7	0	−1	0	+1
	12 months	−2	−3	0	0	0	0	0	−1	−4	−5	−2	−3
SOI$_3$ and SRI$_3$	Concurrent	0	0	0	0	0	0	0	0	0	0	0	0
	3 months	0	0	0	0	0	0	−1	0	0	0	0	0
	6 months	0	+1	0	0	0	0	0	−2	−1	−6	0	0
	12 months	−6	−6	−1	−1	0	0	0	0	0	−4	−6	−6
SOI$_6$ and SRI$_6$	Concurrent	0	0	0	0	0	0	0	0	0	0	0	0
	3 months	0	0	0	0	0	0	0	−2	0	0	0	0
	6 months	0	0	0	0	0	0	0	−1	−1	−2	−2	0
	12 months	−7	−7	−4	−1	−1	0	0	0	0	0	0	−1
SOI$_{12}$ and SRI$_{12}$	concurrent	0	0	0	0	0	0	0	0	−1	0	0	0
	3 months	0	0	0	0	0	0	0	0	−1	−1	−1	0
	6 months	−2	−2	0	0	0	0	0	0	0	−1	−1	−1
	12 months	0	0	0	−1	−2	0	−1	0	−1	−1	−1	−1

The negative number means that there are the corresponding number of stations exhibited significant negative correlations, while the positive number means significant positive correlations

the number of stations exhibited significant correlations increased with the increase in time lag.

On the whole, the results indicate that the direct linkage between SRI and SOI is generally weaker than the corresponding associations with AMOI in the Luanhe River basin, whereas increasing time lags can improve the extent of the linkage. Especially for the time lag of 12 months, the possible influences of ENSO on the drought severity in the basin are evident in winter and spring (September through February).

These findings are consistent with previous researches that have demonstrated the great associations between ENSO events and hydrological variables (temperature and precipitation) in North China at 1- to 6-month lagged stage (Wang 2013), as well as the high correlations between 12-month leading SOI and drought indices of North China (Su and Wang 2007).

4.3 Climate-induced influences

The climate-induced influence indices were calculated for each rain gauge and each time scale (Figs. 3, 4). For all the time scales, the influence frequencies (I_F) averaged over the 21 stations in El Niño and La Niña periods were approximately 50 and 20 %, respectively. Moreover, the influence intensity (I_I) at every station was negative during El Niño phases, while the corresponding one was positive during La Niña phases. The results reveal that El Niño is more strongly correlated with the drought than La Niña, namely El Niño phase might make the drought events prevalent in the study area. For example, most considered stations faced the prolonged droughts at the years during 1982–1983 and 2002–2004 corresponding to the El Niño years. Additionally other extreme and severe droughts (e.g., droughts in 1968, 1972 and 2009) mostly occurred in El Niño phases. Similar associations are found by Chen et al. (1995) and Xia (2003) who indicated that the El Niño phases favor drought conditions in North China.

During the warm phase of AMO, the I_F ranging from 60 to 100 % and the negative I_I were observed at all the stations and all the time scales (Figs. 3, 4). In addition, all the influence indices in warm AMO phases were greater than those in El Niño phases. It is indicated that in the Luanhe River basin, warm AMO episodes are in closer relation with drier conditions, while cold AMO episodes are in closer relation with wetter conditions. Moreover, the results also demonstrate that the potential influence of AMO on the drought
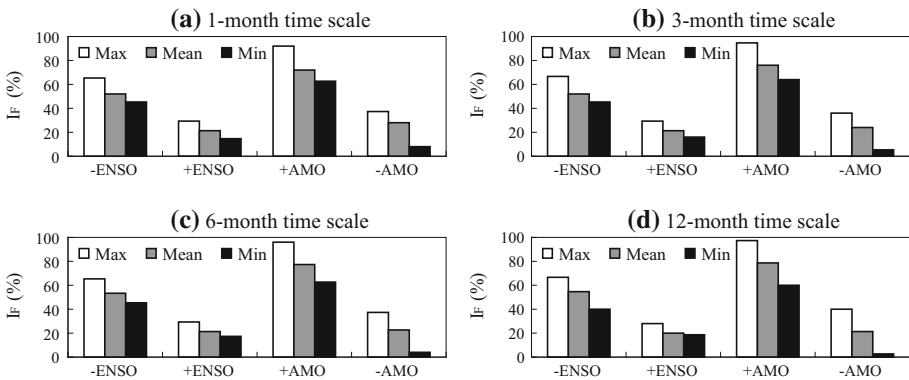

Fig. 3 Maximum, minimum and mean of the influence frequencies (I_F) for all the stations. *Note* −ENSO: El Niño phases; +ENSO: La Niña phases; +AMO: warm AMO phases; −AMO: cold AMO phases
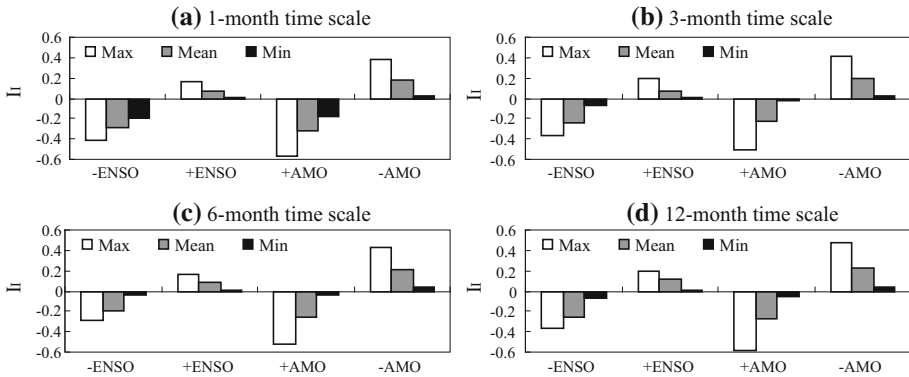
Fig. 4 Maximum, minimum and mean of the influence intensities (I_I) for all the stations. *Note* −ENSO: El Niño phases; +ENSO: La Niña phases; +AMO: warm AMO phases; −AMO: cold AMO phases

is greater than that of ENSO. Therefore, if AMO is to evolve and persist in its positive phase, then the drought in this basin might be enhanced, in terms of both severity and frequency. For instance, the AMO index during 1995 to 2011 exhibited warm anomalies, and the drought events occurred in this period were both large in scale and severe. Previous studies also revealed that the warm phase of AMO acts as a forcing on the substantial East Asian warming in the recent two decades (Li et al. 2009; Wang et al. 2009), which is responsible in part for the dry trend in North China (Ma and Ren 2007; Wang et al. 2010).

4.4 Human-induced influences

Owing to the rapid socioeconomic development and climate change, runoff in the Luanhe River basin has dramatically decreased since the 1980s, along with the frequent occurrence of extreme drought events (Ma et al. 2010; Wang et al. 2013). Human activities, including agricultural irrigation, soil and water conservation works, hydraulic projects and land cover and land use changes, have direct or indirect influences on hydrological drought in the basin. In order to identify the change-point reflecting the influences of human activities, DCC method was conducted between annual precipitation and runoff over eight selected sub-basins. The double cumulative curves of Luanhe and Liuhe sub-basins are shown in Fig. 5 as examples. The results indicate that the original relationship between precipitation and runoff for the basin was broken obviously in 1979. This finding is consistent with previous studies in which (Liu et al. 2013; Wang et al. 2013) demonstrated that 1979 is the abrupt change-point reflecting the impact of human activities on runoff in the Luanhe River basin. Hence, the change-point associated with significant human activities was identified as 1979 in this study, and then the whole study period was divided into two parts: natural period (1958–1979) and impact period (1980–2011).

Corresponding to the hydrological drought index (SRI), the SPI was constructed using the gamma distribution to quantify the status of meteorological drought. The change ratios of meteorological and hydrological drought (R_P and R_R) were calculated over various time scales for each sub-basin, as well as the human-induced influence index (ΔR) (listed in Table 5).

The positive R_P and R_R observed in all the sub-basins, mean that meteorological drought in the Luanhe River basin during the impact period was aggravated compared with that
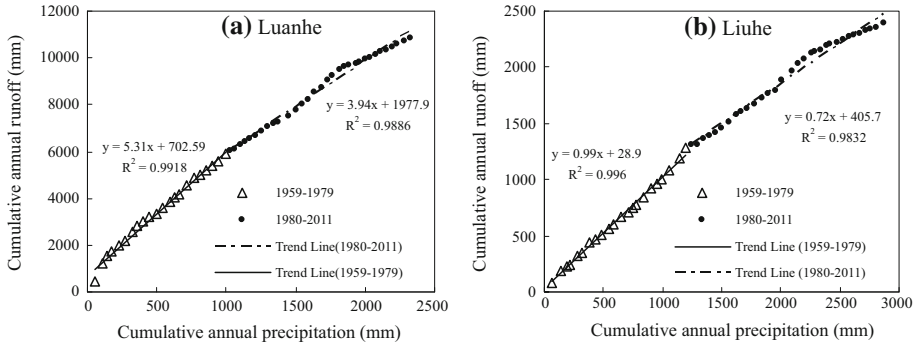
Fig. 5 Double cumulative curves of annual precipitation and runoff for **a** Luanhe and **b** Liuhe sub-basins

during the natural period, and the same trend was seen for the hydrological drought of the basin. This aggravation trend of drought condition is in agreement with those obtained in previous studies (Yin 2013; Shi 2013). The results also indicate that climate anomalies (mainly precipitation change) exert aggravating effects on the drought conditions; thereby, it can be reasonably inferred that the hydrological droughts in the Luanhe River basin would still have become more severe even without the intensive human activities from 1980 to 2011.

The maximum mean R_P was found at 12-month time scale. It means that changes in the meteorological drought at 12-month time scale seem to be more sensitive to the precipitation variability, as compared with other considered time scales. Moreover, the maximum mean R_R occurred at the time scale of 6 months, suggesting that the combined influence of climate changes and human activities might be more significant on the hydrological drought at 6-month time scale.

For 1- and 3-month time scales, a positive ΔR was evident at all the stations, whereas, for the time scale of 6 and 12 months, a negative ΔR was observed at three and five stations, respectively. It implies that the hydrological drought at shorter time scales might be aggravated by other factors (anthropogenic activities) besides the climate change during the period of 1980–2011. However, in respect to the hydrological drought at longer time scales, human activities might have mitigating effects in some areas of the basin.

In order to elucidate these anthropogenic effects in detail, the results in Table 4 were explained and verified with the previous references and past human activities occurred in the basin as follows.

The northwest of Luanhe sub-basin and the entire Xiaoluanhe sub-basin is located at the upper reaches of the study area, where a major population growth occurred during the impact period, along with a conversion of natural grass land to forest land in its northern part (Xu 2009; Shi 2013; Lu 2010). It could be inferred that the increase in water consumption, caused by population expansion, generates the aggravating effect on hydrological drought for all the time scales in Xiaoluanhe sub-basin. Owing to the increased forest cover, the runoff reduction on monthly or seasonal time scale is particularly strong through the increase in evapotranspiration and interception, but runoff increase at annual even longer time scale has been primarily resulted from the increased groundwater contribution (Iroumé et al. 2005; Shao et al. 2009; Ye et al. 2013; Zhang et al. 2014). Therefore, the human activities showing the mitigating effect at 12-month time scale in Luanhe sub-basin is mainly associated with the afforestation in northern Luanhe sub-basin.

Table 5 Change ratios of drought (R_P and R_R) and human-induced influence index (ΔR) at 4 time scales for the 8 sub-basins

Time scale	1 month			3 months			6 months			12 months		
Indices (%)	R_P	R_R	ΔR	R_P	R_R	ΔR	R_P	R_R	ΔR	R_P	R_R	ΔR
Sub-basin												
Luanhe	9.10	16.51	7.41	14.73	20.69	5.95	7.63	19.39	11.77	26.85	17.79	−9.06
Wuliehe	5.13	22.47	17.33	10.51	22.67	12.16	3.87	22.77	18.90	10.64	26.06	15.42
Baohe	1.97	6.14	4.17	2.18	10.37	8.19	3.16	12.47	9.31	11.48	2.57	−8.92
Xiaoluanhe	1.69	2.89	1.21	2.27	12.63	10.36	5.54	16.77	11.23	8.11	19.17	11.06
Yimatuhe	2.60	18.53	15.93	10.86	21.87	11.01	14.31	11.61	−2.70	20.47	16.18	−4.30
Laoniuhe	7.64	27.98	20.35	5.77	47.74	41.97	5.45	48.98	43.53	14.53	37.79	23.25
Xingzhouhe	3.32	7.13	3.82	9.07	12.82	3.75	9.66	7.23	−2.43	21.35	8.84	−12.51
Liuhe	5.92	8.15	2.23	5.80	6.78	0.98	12.94	9.38	−3.56	17.21	12.18	−5.03

The middle part of the study area, including Yimatuhe, Xingzhouhe, Wuliehe and the southeast of Luanhe sub-basins, has a significant change in land use, namely large expanses of natural forest were transformed into grassland and urban area after 1980 (Shi 2013; Dong 2013; Bao et al. 2012). The deforestation could have the potential to enhance the magnitude of drought on seasonal time scale (Snyder 2010; Bagley et al. 2011, 2014), corresponding to the human-induced aggravating effects observed in this region at shorter time scales. The development of economy, industry and urbanization in this region accelerated at the start of the 1980s, which coincided with China's reform and opening-up policy occurred in 1979 (Ren et al. 2002; Yuan et al. 2005). Accordingly, the increase in water demand for industrial production, daily life and municipal engineering during the impact period, directly led to a rapid increase in the amount of surface water withdrawal and groundwater exploitation (Ma et al. 2010; Wang et al. 2013). The related water use was capable of exacerbating the hydrological droughts at various time scales in the region. Furthermore, a lot of mini dams have been constructed since 1980s over the region to control the soil erosion (Gao et al. 2002; Wang and Wang 2009). That would enhance infiltration and limit direct runoff, consequently leading to a decrease in the peak discharge and an increase in the amount of base flow (Maidment 1993; Bao et al. 2012). This diminished variability of runoff emerges as the possible explanation for the human-induced mitigation of hydrological drought at longer time scales in the Yimatuhe and Xingzhouhe sub-basins.

In the downstream region, consisting of Liuhe, Laoniuhe and Baohe sub-basins, there is extensive evidence for the increased agricultural activity resulted from the China's land reform policy in 1978 (Yang and Tian 2009; Bao et al. 2012). The expansion of agricultural land and increased agricultural water use consequently happened in this region during the impact period (Shi 2013; Dong 2013; Wang et al. 2013), which were considered as the most probable driving factors for the human-induced aggravation of hydrological drought at short time scales. However, the dynamics of low-flow regimes were altered by the enhanced farmland irrigation, since most irrigation water seeped into the ground and ultimately contributed to base flow (Schilling 2004; Tomer et al. 2005; Zhang et al. 2011). This alteration could be responsible for the increased streamflow during the dry season (Ye et al. 2013; Wang and Cai 2009), and partially explain the mitigating effect on hydrological drought at longer time scales observed in Liuhe and Baohe sub-basins.

The ΔR of the Laoniuhe sub-basin was greater than that of other sub-basins over all the time scales. It indicates that the aggravation of hydrological drought in this sub-basin is mainly governed by human activities. Especially the extensive urbanization, which causes a large increase in water withdrawal and high percent urban area within the sub-basin, might be regarded as the major driving factor exacerbating the regional drought condition. It agrees with the conclusions of Wang et al. (2013) and Shi (2013), who found that the runoff reduction, as well as the drought aggravation during the impact period, was primarily attributed to the anthropogenic forces in the Luanhe River basin.

In addition, the Liuhe sub-basin with the smallest 3-month ΔR suggested that, the associated human activities of this sub-basin indeed made a relatively small contribution to the aggravation of hydrological droughts at 3-month time scale. This slight contribution is inconsistent with the fact that the regional agricultural expansion occurred intensely during the impact period (Li et al. 2014). It might be explained by the diverse human-induced effects which counteract each other concurrently at seasonal time scale.

5 Discussions and conclusions

This study analyzed hydrological droughts in the Luanhe River basin and their associations with large-scale climate patterns (ENSO and AMO) during 1959–2011, then developed influence indices based on SRI and SPI to detect the possible influences of climate anomalies and human activities on the hydrological droughts at various time scales. Some conclusions and associated discussions are as follows.

1. The SRI is found to be a useful tool for monitoring hydrological drought events, and analysis results based on the SRI are in good agreement with the previously published descriptions of droughts in the Luanhe River basin. The results in this study also demonstrate that the drought conditions of the basin have become more severe during the last decade.

Due to its flexibility to observe different time scales and its standardization, the SRI is capable of capturing both short- and long-term droughts. As a runoff-based index, the SRI on various time scales can not only represent the deficits in different water sources (e.g., soil moisture, reservoir and groundwater), but also express the status of water utilization over the related time period in a region. The SRI at shorter time scale changes sensitively in response to emerging hydrological droughts, and thus is important to agricultural interests. In addition, the efficacy of the SRI at longer time scale for reflecting a prolonged hydrological drought may be of significant interests to water supply managers. Therefore, the examination of multiple SRIs with various time scales can provide valid information of the overall drought status and valuable references for drought monitor and assessment.

2. The results of correlation analyses indicate that the significant influence of AMO on hydrological drought is evident across the Luanhe River basin. As for the hydrological drought at different time scales, the potential teleconnection of AMO occurs among different months, especially in July and August. In response to ENSO, the direct linkage between the SRI and SOI during the study period is generally weaker than the corresponding association with AMOI, while the extent of the linkage can be improved with increasing time lags. These findings can provide opportunities for improving predictability of drought in the basin by taking into account changes of large climate patterns.

Nevertheless, the weak SRI-SOI correlation discovered in this study does not mean that ENSO has a slight effect on the hydrological drought of the basin, because Kendall's τ test just evaluates the strength of monotonic correlation between two variables. Namely, significant correlations do not imply the existence of a causal dependency, only providing a measure of the association between the variables over time. So the weak correlation might suggest that the SRI-SOI relationship is likely to be non-monotonic. Moreover, many former researchers indicated that ENSO exerts different impacts on drought conditions in different regions of China (Yin et al. 2009; Jiang et al. 2006). Ropelewski and Halpert (1986) pointed out that the regions without consistent ENSO-related signals might indirectly feel the effects of the ENSO cycle through the position of other ENSO-related phenomenon. Therefore, further examination of other factors is needed to explain the relationship between the ENSO and hydrological drought in the Luanhe River basin.

3. Based on the climate-induced influence indices, the effects of climate phases on regional drought condition were examined with respect to the intensity and frequency. The analyses conducted in this study reveal that warm AMO phases favor drought

conditions and El Niño phases show a close relation with drought events in the Luanhe River basin. This conclusion agrees with the previous studies which indicated that during the typical warm phase of ENSO, surface conditions are drier in most regions of China, especially in North China (Su and Wang 2007; Ouyang et al. 2014).

More attention should be paid on the weaker teleconnection of ENSO obtained in this study as compared with that of AMO. Yin et al. (2009) also found the weakening linkage between ENSO and flood/drought change of the Taihu Lake basin in China during recent decades, and it is speculated that this weakening association might relate to the cold and warm inter-decadal background (Chang et al. 2001; Gao and Wang 2007). What's more, the warm AMO phase may have been responsible in part for the substantial East Asian warming in the recent two decades (Wang et al. 2009). It is well known that Eastern Asian summer and winter monsoons are influenced by El Niño and La niña, meanwhile warm-phase AMO intensifies the East Asian summer monsoon but weakens the winter monsoon. Thus, AMO to some extent can modulate the influence of ENSO on regional drought condition, and the effects of combining different phases of AMO and ENSO need to be further studied.

4. The human-induced influence index developed in this study provides a way to identify the impacts of human activities on drought. It is implied that at shorter time scales, human activities make a contribution to the aggravation of hydrological droughts over the Luanhe River basin. However, at longer time scales, human activities might show mitigating effects on hydrological droughts in some areas of the basin.

As mentioned earlier, different economic and social sectors pay attention to the hydrological drought at different time scales. The results related to human-induced effects over various time scales could provide valuable references for future water resources planning and management decisions to support sustainable water resources development at catchment scale.

Human activities, including agricultural irrigation, soil and water conservation works and land cover and land use changes, have direct or indirect influences on the hydrological drought of the basin. The effects of the various forms of human activity might accumulate or counteract each other simultaneously. So the human-induced mitigating or aggravating effect assessed in this study is a comprehensive response to the hydrological drought. In reality, there were still some anthropogenic disturbances (such as farmland irrigation and land cover changes) even during the natural period. Additionally, it should be noted that the climate-induced effect defined in this study is purely related to precipitation variations, ignoring the impacts from other climate variables such as evaporation. Therefore, this study just did some rough estimations, and quantitative analyses should be investigated in future studies.

References

Bagley JE, Desai AR, West PC et al (2011) A simple, minimal parameter model for predicting the influence of changing land cover on the land–atmosphere system. Earth Interact. doi:10.1175/2011EI394.1

Bagley JE, Desai AR, Harding KJ et al (2014) Drought and deforestation: has land cover change influenced recent precipitation extremes in the Amazon? J Clim 27(1):345–361

Bao ZX, Zhang JY, Wang GQ et al (2012) Attribution for decreasing streamflow of the Haihe River basin, northern China: climate variability or human activities? J Hydrol 460:117–129

Beran M, Rodier J (1985) Hydrological aspects of drought: a contribution to the international hydrological programme. Vol 39 of Studies and Reports in Hydrology. Unesco-WMO, Paris, France

Bolboaca SD, Jäntschi L (2006) Pearson versus Spearman, Kendall's tau correlation analysis on structure–activity relationships of biologic active compounds. Leonardo J Sci 9:179–200

Bordi I, Sutera A (2001) Fifty years of precipitation: some spatially remote teleconnnections. Water Resour Manag 15(4):247–280

Bradbury JA, Dingman SL, Keim BD (2002) New England drought and relations with large scale atmospheric circulation patterns. JAWRA 38(5):1287–1299

Chang CP, Patrick H, Ju JH (2001) Possible roles of Atlantic circulations on the weakening Indian monsoon rainfall–ENSO relationship. J Clim 14(11):2376–2380

Chen ZH, Yang GF (2013) Analysis of drought hazards in North China: distribution and interpretation. Nat Hazards 65:279–294

Chen JY, Drosdowsky W, Nicholls N (1995) A study of teleconnections between regional floods/droughts in China for flood season and ENSO events. J Cent Univ Natl (Natural Sciences Edition) 4(1):41–50 (in Chinese)

Croux C, Dehon C (2010) Influence functions of the Spearman and Kendall correlation measures. Stat Methods Appl 19:497–515

Di Rita F, Magri D (2009) Holocene drought, deforestation and evergreen vegetation development in the central Mediterranean: a 5500 year record from LagoAlimini Piccolo, Apulia, southeast Italy. The Holocene 19(2):295–306

Dong GQ (2013) Attribution study based on ensemble simulation of the evolution of water resources in Luanhe River basin. Donghua University, Shanghai (in Chinese)

Dracup JA, Lee KS, Paulson EG Jr (1980) On the definition of droughts. Water Resour Res 16(2):297–302

Enfield DB, Mestas-Nunez AM, Trimble PJ (2001) The Atlantic multidecadal oscillation and its relation to rainfall and river flow over the U.S. Geophys Res Lett 28:2077–2080

Feng P, Hu R, Li JZ (2014) Meteorological drought grade prediction using three-dimensional log-linear models. J Hydraul Eng 45(5):505–512 (in Chinese)

Fraedrich K, Müller K (1992) Climate anomalies in Europe associated with ENSO extremes. Int J Climatol 12(1):25–31

Gao H, Wang YG (2007) On the weakening relationship between summer precipitation and ENSO. Acta Meteorol Sin 65(1):131–137 (in Chinese)

Gao YC, Yao ZJ, Liu BQ et al (2002) Evolution trend of Miyun reservoir inflow and its motivating factors analysis. Prog Geogr 21:546–553 (in Chinese)

Hosseinzadeh Talaee P, Tabari H, SobhanArdakani S (2012) Hydrological drought in the west of Iran and possible association with large-scale atmospheric circulation patterns. Hydrol Process 28(3):764–773

Iroumé A, Huber A, Schulz K (2005) Summer flows in experimental catchments with different forest covers, Chile. J Hydrol 300(1):300–313

Jiang T, Zhang Q, Zhu DM et al (2006) Yangtze floods and droughts (China) and teleconnections with ENSO activities (1470–2003). Quat Int 144(1):29–37

Kao SC, Govindaraju RS (2010) A copula-based joint deficit index for droughts. J Hydrol 380(1):121–134

Kerr RA (2000) A north Atlantic climate pacemaker for the centuries. Science 288(5473):1984–1986

Kim TW, Valdés JB, Nijssen B et al (2006) Quantification of linkages between large-scale climatic patterns and precipitation in the Colorado River basin. J Hydrol 321(1):173–186

Kirono DGC, Kent DM, Hennessy KJ et al (2011) Characteristics of Australian droughts under enhanced greenhouse conditions: results from 14 global climate models. J Arid Environ 75(6):566–575

Knight JR, Folland CK, Scaife AA (2006) Climate impacts of the Atlantic multidecadal oscillation. Geophys Res Lett 33:L17706. doi:10.1029/2006GL026242

Li SL, Bates GT (2007) Influence of the Atlantic multidecadal oscillation on the winter climate of East China. Adv Atmos Sci 24(1):126–135

Li JZ, Feng P (2007) Runoff variations in the Luanhe river basin during 1956–2002. J Geogr Sci 17:339–350

Li LJ, Zhang L, Wang H et al (2007) Assessing the impact of climate variability and human activities on streamflow from the Wuding River basin in China. Hydrol Process 21:3485–3491

Li SY, Wang YM, Gao YQ (2009) A review of the researches on the Atlantic multidecadal oscillation (AMO) and its climate influence. Trans Atmos Sci 32(3):458–465 (in Chinese)

Li S, Xiong L, Dong L et al (2013) Effects of the Three Gorges Reservoir on the hydrological droughts at the downstream Yichang station during 2003–2011. Hydrol Process 27(26):3981–3993

Li JZ, Tan SM, Chen FL et al (2014) Quantitatively analyze the impact of land use/land cover change on annual runoff decrease. Nat Hazards 74(2):1191–1207

Liu XF, Xiang L, Zhai JQ (2013) Quantitative study of impacts for environmental change on runoff in Luanhe River basin. J Nat Resour 28(2):244–252 (in Chinese)

López-Moreno JI, Vicente-Serrano SM, Beguería S et al (2009) Dam effects on droughts magnitude and duration in a transboundary basin: the Lower River Tagus, Spain and Portugal. Water Resour Res 45(2):W02405. doi:10.1029/2008WR007198

Lu ML (2010) Feature of land use change and analysis of its changing trend in Haihe River basin. Tianjin University, Tianjin (in Chinese)

Lu AG, Ge JQ, Pang DQ et al (2006a) Asynchronous response of droughts to ENSO in China. J Claciol Geocryol 28(4):535–542 (in Chinese)

Lu R, Dong B, Ding H (2006b) Impact of the Atlantic multidecadal oscillation on the Asian summer monsoon. Geophys Res Lett 33:L24701. doi:10.1029/2006GL027655

Ma ZG, Ren XB (2007) Drying trend over China from 1951 to 2006. Adv Clim Change Res 3(4):195–201 (in Chinese)

Ma H, Yang D, Tan SK et al (2010) Impact of climate variability and human activity on streamflow decrease in the Miyun Reservoir catchment. J Hydrol 389(3):317–324

Ma HJ, Yan DH, Weng BS et al (2013) Applicability of typical drought indexes in the Luanhe River basin. Arid Zone Res 30(4):728–734 (in Chinese)

Maidment DR (1993) Handbook of hydrology. R.R. Donnelley, USA

McKee TB, Doesken NJ, Kleist J (1993) The relationship of drought frequency and duration to time scales. In: Proceedings of the 8th conference on applied climatology. American Meteorological Society, Boston, MA, vol 17(22), pp 179–183

Mo KC, Schemm JKE, Yoo SH (2009) Influence of ENSO and the Atlantic multidecadal oscillation on drought over the United States. J Clim 22(22):5962–5982

Nalbantis I, Tsakiris G (2009) Assessment of hydrological drought revisited. Water Resour Manag 23:881–897

Nicholls N (2004) The changing nature of Australian droughts. Clim Change 63:323–336

Niehoff D, Fritsch U, Bronstert A (2002) Land-use impacts on storm-runoff generation: scenarios of land-use change and simulation of hydrological response in a meso-scale catchment in SW-Germany. J Hydrol 267(1):80–93

Ouyang R, Liu W, Fu G et al (2014) Linkages between ENSO/PDO signals and precipitation, streamflow in China during the last 100 years. Hydrol Earth Syst Sci Discus 11(4):4235–4265

Özger M, Mishra AK, Singh VP (2009) Low frequency drought variability associated with climate indices. J Hydrol 364(1):152–162

Ren LL, Wang MR, Li CH et al (2002) Impacts of human activity on river runoff in the northern area of China. J Hydrol 261:204–217

Ropelewski CF, Halpert MS (1986) North American precipitation and temperature patterns associated with the El Nino/southern oscillation (ENSO). Mon Weather Rev 114:2352–2362

Schilling KE (2004) Relation of baseflow to row crop intensity in Iowa. Agric Ecosyst Environ 105:433–438

Searcy JK, Hardison CH (1960) Double-mass curves. US Geol Surv Water Supply Pap 1541:31–66

Shao QX, Zhang L, Chen YD, Singh VP (2009) A new method formodeling flow duration curves and predicting streamflow regimes under altered land use conditions. Hydrol Sci J 54(3):606–622

Shi XL (2013) Study on distributed hydrological simulation and drought evaluation method in Luanhe River basin based on SWAT model. University of Chinese Academy of Sciences, Beijing (in Chinese)

Shukla S, Wood AW (2008) Use of a standardized runoff index for characterizing hydrologic drought. Geophys Res Lett. doi:10.1029/2007GL032487

Snyder P (2010) The influence of tropical deforestation on the Northern Hemisphere climate by teleconnections. Earth Interact. doi:10.1175/2010EI280.1

Sol'áková T, De Michele C, Vezzoli R (2014) Comparison between parametric and nonparametric approaches for the calculation of two drought indices: SPI and SSI. J Hydrol Eng 19(9). doi:10.1061/(ASCE)HE.1943-5584.0000942

Song XM, Zhang JY, Zhan CS et al (2013) Review for impacts of climate change and human activities on water cycle. J Hydraul Eng 44(7):779–790 (in Chinese)

Stahl K, Demuth S (1999) Linking streamflow drought to the occurrence of atmospheric circulation patterns. Hydrol Sci J 44(3):467–482

Su HX, Li GQ (2012) Low-frequency drought variability based on SPEI in association with climate indices in Beijing. Acta Ecol Sin 32(17):5467–5475 (in Chinese)

Su MF, Wang HJ (2007) Relationship and its instability of ENSO—Chinese variations in droughts and wet spells. Sci China Ser D Earth Sci 50(1):145–152

Sutton RT, Hodson DLR (2005) Atlantic Ocean forcing of North American and European summer climate. Science 309:115–118

Tang XC, Yuan ZY (2010) The influence of the drought disaster caused by El Nino events in Guangdong Province in recent 60 years. Geogr Res 29(11):1932–1939 (in Chinese)

Tomer MD, Meek DW, Kramer LA (2005) Agricultural practices influence flow regimes of headwater streams in western Iowa. J Environ Qual 34(5):1547–1558

Troup AJ (1965) The southern oscillation. Quart J R Meteorol Soc 91:490–506

van Huijgevoort MHJ, Hazenberg P, van Lanen HAJ, Uijlenhoet R (2012) A generic method for hydrological drought identification across different climate regions. Hydrol Earth Syst Sci Discus 9:2033–2070

Vasiliades L, Loukas A, Liberis N (2011) A water balance derived drought index for Pinios River basin, Greece. Water Resour Manag 25:1087–1101

Wang H (2013) Climate change around Bohai region during 1956 to 2011 and its relationship with ENSO. Northwest Normal University Lanzhou, Lanzhou (in Chinese)

Wang DB, Cai XM (2009) Detecting human interferences to low flows through base flow recession analysis. Water Resour Res 45:W07426. doi:10.1029/2009WR007819

Wang Q, Wang C (2009) Impact of human activity on runoff in Haihe River basin. Haihe Water Resour 1:4–6 (in Chinese)

Wang HJ, Yang ZS, Saito Y et al (2006) Interannual andseasonal variation of the Huanghe (Yellow River) water dischargeover the past 50 years: connections to impacts from ENSO eventsand dams. Global Planet Change 50:212–225

Wang YM, Li SL, Luo DH (2009) Seasonal response of Asian monsoonal climate to the Atlantic multidecadal oscallation. J Geophys Res 114:1–15. doi:10.1029/2008JD010929

Wang JS, Chen FH, Jin LY et al (2010) Characteristics of the dry/wet trend over arid central Asia over the past 100 years. Clim Res 41(1):51–59

Wang W, Shao Q, Yang T et al (2013) Quantitative assessment of the impact of climate variability and human activities on runoff changes: a case study in four catchments of the Haihe River basin, China. Hydrol Process 27(8):1158–1174

Wen L, Rogers K, Ling J, Saintilan N (2011) The impacts of river regulation and water diversion on the hydrological droughts characteristics in the Lower Murrumbidgee River, Australia. J Hydrol 405:382–391

Xia DD (2003) The study on the global land precipitation associated with ENSO during 1920–2000. Nanjing Institute of Meteorology, Nanjing (in Chinese)

Xing ZQ, Yan DH, Lu F et al (2013) Advances in the study of anthropogenic effects on the drought and flood events. J Nat Resour 28(6):1070–1082 (in Chinese)

Xiong LH, Guo SL (2004) Trend test and change-point detection for the annual discharge series of the Yangtze River at Yichang hydrological station. Hydrol Sci J 49(1):99–112

Xu XG (2009) Research on optimal operation of joint water supply of reservoir group in middle-down streams of Luan River. Tianjin University, Tianjin (in Chinese)

Yang YH, Tian F (2009) Abrupt change of runoff and its major driving factors in Haihe River Catchment, China. J Hydrol 374:373–383

Yang ZY, Yuan Z, Fang HY et al (2013) Study on the characteristic of multiply events of drought and flood probability in Luanhe River basin based on Copula. J Hydraul Eng 44(005):556–561 (in Chinese)

Ye XC, Zhang Q, Liu J et al (2013) Distinguishing the relative impacts of climate change and human activities on variation of streamflow in the Poyang Lake catchment, China. J Hydrol 494:83–95

Yin J (2013) Evolution law and comprehensive measures of drought of mountain area in Haihe basin. China Institute of Water Resources & Hydropower Research, Beijing (in Chinese)

Yin Y, Xu Y, Chen Y (2009) Relationship between flood/drought disasters and ENSO from 1857 to 2003 in the Taihu Lake basin, China. Quat Int 208(1):93–101

Yuan F, Xie ZH, Liu Q et al (2005) Simulating hydrologic changes with climate change scenarios in the Haihe River basin. Pedosphere 15(5):595–600

Zeng SD, Xia J, Du H et al (2014) Effects of climate change, land use and cover change and CO_2 enrichmenton runoff: a case study of the Luanhe River basin. Adv Water Sci 25(1):10–20 (in Chinese)

Zhang YF, Guan DX, Jin CJ et al (2011) Analysis of impacts of climate variability and human activity on streamflow for a river basin in northeast China. J Hydrol 410:239–247

Zhang AJ, Zhang C, Fu GB et al (2012) Assessments of impacts of climate change and human activities on runoff with SWAT for the Huifa River basin, Northeast China. Water Resour Manag 26(8):2199–2217

Zhang C, Shoemaker CA, Woodbury JD et al (2013) Impact of human activities on stream flow in the Biliu River basin, China. Hydrol Process 27(17):2509–2523

Zhang C, Wang DG, Wang GL et al (2014) Regional differences in hydrological response to canopy interception schemes in a land surface model. Hydrol Process 28(4):2499–2508

Zhao FF, Xu ZX, Zhang L et al (2009) Streamflow response to climate variability and human activities in the upper catchment of the Yellow River basin. Sci China Ser E Technol Sci 52:1–8